Improvement in Processability of Metallocene Polyethylene by Ultrasound and Binary Processing Aid

Jinyao Chen, Xiaolong Liu, Huilin Li

State Key Laboratory of Polymer Materials Engineering, Polymer Research Institute of Sichuan University, Chengdu, 610065, People's Republic China

Received 5 November 2005; accepted 9 March 2006
DOI 10.1002/app.24506
Published online in Wiley InterScience (www.interscience.wiley.com).

ABSTRACT: The effect of ultrasonic vibration and binary processing aid in improving the processability of metallocene linear low-density polyethylene (mLLDPE) was investigated. During extrusion, ultrasonic vibration clearly reduced the die pressure and apparent viscosity of mLLDPE but had only a slight effect on its melt fracture. The effect of diatomite/PEG binary processing aid (BPA) was excellent in reducing the viscosity and eliminating the sharkskin fracture of mLLDPE. The effect of ultrasonic vibration and binary processing aid in improving the processability of mLLDPE was synergetic. With a combination of ultrasonic vibration and a small amount of processing aid, the flowability of mLLDPE was further improved, and the critical shear rate for the onset of sharkskin fracture was increased. © 2006 Wiley Periodicals, Inc. J Appl Polym Sci 103: 1927–1935, 2007

Key words: rheology; polyethylene (PE); processing; viscosity

INTRODUCTION

Metallocene catalyst for the polymerization of olefins has enabled materials to be produced that have a narrow molecular weight distribution (MWD) and a narrow comonomer distribution. Metallocene linear low-density polyethylene (mLLDPE) with narrow MWD possesses better mechanical and optical properties.[1–5] However, mLLDPE with such characteristics is more difficult to be processed than conventional ones.

To improve the processability of mLLDPE, many researchers blended mLLDPE with LDPE, HDPE, and PP.[5,6] And mLLDPE with long-chain branching (LCB) or a bimodal molecular weight distribution was also produced.[2,7–10] Fluoropolymer polymer processing aids (PPAs), which are widely used to improve the processability of LLDPE,[11,12] are also used in mLLDPE.[13,14] Certain fluoropolymers act as die lubricants, allowing the host polymer melts to slip along the die wall, thus delaying the onset of melt flow instability. Boron nitride is also used as a PPA for mLLDPE. It was found that the addition of a small amount of boron nitride eliminated sharkskin melt fracture and postponed the gross melt fracture to a higher shear rate.[15–19] In our previous work, we found that the diatomite/PEG hybrid had a synergetic effect in improving the processability of mLLDPE.[20] A small amount of the diatomite/PEG hybrid dramatically decreased the viscosity of mLLDPE.

Recently, ultrasonic vibrations have been introduced into polymer processing. Isayev et al.[21,22] reported that during extrusion a high-intensity ultrasonic vibration could reduce die pressure and extrudate swelling as well as postpone melt fracture. In our previous work, ultrasonic vibration technology was developed to improve the processability of ultra-high-molecular-weight polyethylene (UHMWPE).[23] In the present study, the processing behavior of mLLDPE resins under ultrasonic vibration was investigated, and the synergetic effect of ultrasonic vibration and diatomite/polyethylene glycol binary processing aid on the processability of mLLDPE is examined.

EXPERIMENTAL

Materials

The metallocene linear low-density polyethylene (mLLDPE, Exceed 1018CA) used in this work, which had a melt flow rate of 1.0 g/10 min (190°C, 2.16 kg), was supplied by Exxon Mobil (Houston, TX). Ziegler–Natta linear low-density polyethylene (ZN-LLDPE)

Correspondence to: H. Li (nic7703@scu.edu.cn).
Contract grant sponsor: National Nature Science Foundation of China; contract grant number: 50233010.
Contract grant sponsor: National Basic Research Program of China; contract grant number: 2005CB623800.
Contract grant sponsor: Funds for Doctoral Disciplines of Ministry of Education of China; contract grant number: 20030610057.

TABLE I
Molecular Structure Parameters

Resin	Density (g/cm^3)	$\bar{M}_w$ (10^{-4} g/mol)	$\bar{M}_w/\bar{M}_n$	MI (g/10 min, 190°C, 2.16 kg)
mLLDPE	0.918	14.30	2.4	1.0
ZN-LLDPE	0.920	14.12	4.33	2.1

with a melt flow rate of 2.0 g/10 min (190°C, 2.16 kg) was obtained from QiLu Petrochemical Corporation (Zibo, China). The molecular structure parameters of mLLDPE and ZN-LLDPE are listed in Table I. Diatomite with a particle size of about 5 μm was supplied by NaHui Desiccating Agent Company (Shanghai, China). Polyethylene glycol (PEG) with a molecule weight of about 6000 was used as additive without further treatment. The diatomite/PEG binary processing aid (BPA) with a ratio of 2 : 1 (w/w) was prepared on a two-roll mill for 20 min at 70°C and then pelletized for further application.

Extrusion under ultrasonic vibration

A special ultrasonic vibration extrusion system developed in our lab was used for the experiment. Its schematic diagram is shown in Figure 1. The die, which was constructed of steel, was a special horn capillary ($L/D = 8$) attached to a single screw extruder. A probe of ultrasonic vibrations with a maximum power output of 300 W and a frequency of 20 kHz was inserted into the polymer melt in the region of the die, and the direction of ultrasonic vibration coincided with that of the melt flow during extrusion. A pressure transducer and a thermal couple at the die entry were installed in order to continuously record the variation in die pressure and temperature during extrusion.

Apparent shear rate ($\dot{\gamma}_a$), wall shear stress (τ_a) and apparent viscosity (η_a) were obtained using the following formulas:

$$\tau_a = \frac{\Delta p D}{4L} \tag{1}$$

$$\dot{\gamma}_a = \frac{32Q}{\pi D^3} \tag{2}$$

$$\eta_a = \frac{\tau_a}{\dot{\gamma}_a} \tag{3}$$

where Q is the volumetric flow rate; D and L are the capillary diameter and length, respectively; and Δp is the pressure drop along the capillary.

Mechanical testing and characterization

Tensile strength was measured with an Instron 4302 universal testing instrument (Instron Co., UK) at a tension speed of 500 mm/min according to GB1040-79.

Capillary rheometer

Rheological measurements were also performed with a constant rate capillary rheometer (Gottfert Rheograph 2002, Germany) whose capillary diameter, D, and length-to-diameter ratio, L/D, were 1 mm and 30, respectively. The flow properties of these specimens were measured over an apparent shear rate range of 10–3000 s^{-1} at different temperatures. Test samples for capillary rheology analysis were prepared on a two-roll mill for 10 min at 120°C.

Dynamic rheological properties

The frequency sweep dynamic rheology experiments of the melt samples were carried out on an Advanced Rheometrics Expansion System (ARES-9A, Rheometrics Co., USA) using the dynamic oscillatory mode with a 25-mm parallel plate fixture. The frequency ranged from 0.25 to 100 Hz. Test samples were molded into a circular disk 2 mm thick and 25 mm in diameter at 190°C. Sample response linearity with respect to temperature was verified, and nitrogen gas was used to prevent thermal oxidation.

Thermal analysis

Thermal analysis of the materials was carried out in a Netzsch DSC 204 differential scanning calorimeter (Netzsch Co., Germany). All samples were first heated to 150°C and held at that temperature for 5 min. Then the samplers were cooled at various rates (2.5, 5, 10, 15, or 20°C/min) to 30°C and held at that temperature for 5 min. They were then scanned from 30°C to 150°C at a rate of 10°C/min. Crystallization and melting temperature were obtained from the cooling and second-heating thermograms, respectively.

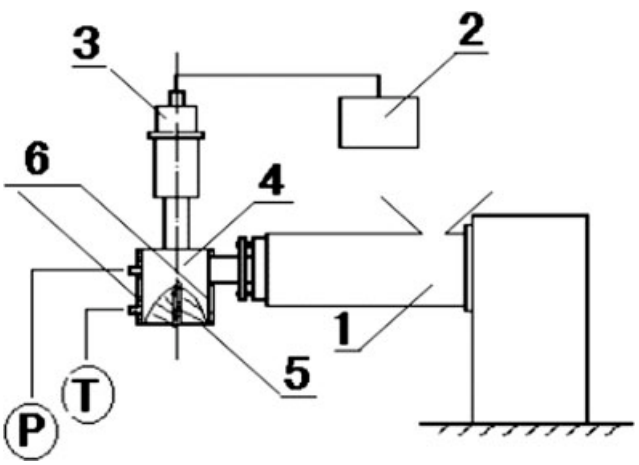

Figure 1 Scheme of ultrasonic–extrusion system: (1) extruder, (2) ultrasonic generator (3) piezoelectric transducer, (4) die, (5) melt, (6) electric heaters, P, pressure transducer; T, thermocouple.

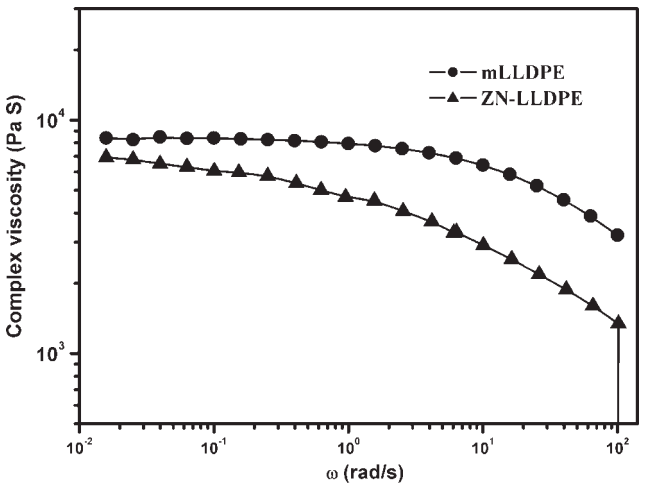

Figure 2 Complex viscosity of mLLDPE and ZN-LLDPE at 190°C.

X-ray diffraction

The WAXD patterns of samples were taken on a Philip X'pert prd diffractometer (Japan) with Ni-filtered Cu Kα radiation at room temperature. The accelerating voltage and electric current used were 50 kV and 30 mA, respectively. The scanning angular degree ranged from 10 to 40 (2θ).

RESULT AND DISCUSSION

Dynamic rheological properties of mLLDPE and ZN-LLDPE

Figure 2 shows the relationship of complex viscosity, η*, to frequency, ω, for mLLDPE and ZN-LLDPE at 190°C. ZN-LLDPE and mLLDPE have similar weight-average molecular weights, but ZN-LLDPE, which had a broader MWD and long chain branching (LCB), showed greater shear-shinning behavior. Therefore, ZN-LLDPE had lower viscosity at a higher frequency or a higher shear rate, whereas, because of its narrow-molecular-weight distribution, mLLDPE had little shear-shinning behavior. The viscosity of mLLDPE was much larger than that of ZN-LLDPE, making mLLDPE difficult to be processed.

The dependence of storage and loss moduli of mLLDPE and ZN-LLDPE on frequency, ω, at 190°C is shown in Figure 3. The storage modulus increased with an increase in frequency. At a low frequency ZN-LLDPE showed higher storage modulus because of the presence of LCB, but this behavior changed as the frequency increased. The storage modulus of mLLDPE was higher than that of ZN-LLDPE at high frequencies. The loss modulus increased with an increase in frequency, and the loss modulus of mLLDPE was higher than that of ZN-LLDPE over all frequencies.

Effect of ultrasonic vibration on extrusion behavior of mLLDPE

The relative decrease in die pressure, ΔP, induced by ultrasonic vibrations during extrusion was quantified by:

$$\Delta P\% = (P_0 - P_i)/P_0 \times 100\% \quad (4)$$

where P_0 and P_i are the die pressures in the absence and in the presence of ultrasonic vibrations, respectively. Die pressure changes with ultrasonic vibration intensity were measured at a die temperature of 180°C.

The presence of ultrasonic vibrations increased the drop in the die pressure of mLLDPE melt during extrusion, as shown in Figure 4. ΔP showed an almost linear increase with an increase in ultrasonic intensity. When the ultrasonic intensity was 200 W, the decrease in die pressure, ΔP, was 28.94% at a screw rotation speed of 10 rpm. This indicates that the die pressure of mLLDPE can be decreased in the presence of ultrasonic vibrations.

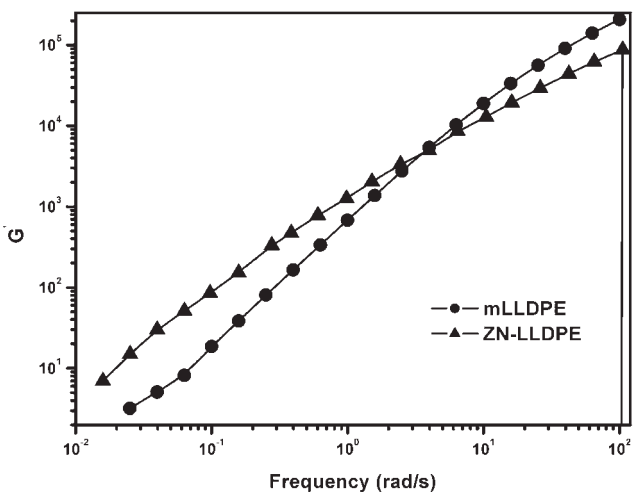

(a)

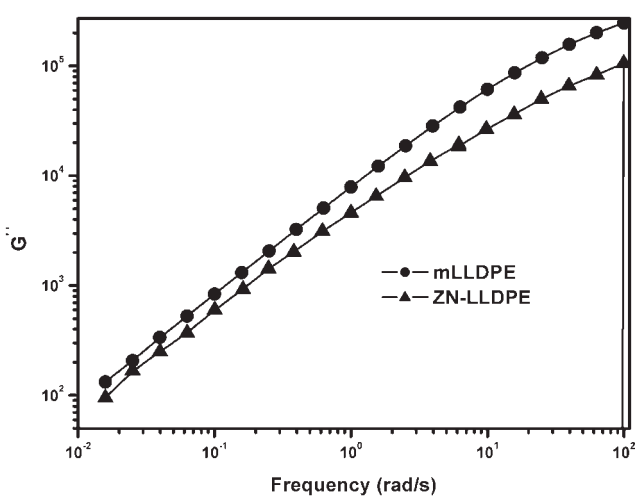

(b)

Figure 3 Dynamic moduli of mLLDPE and ZN-LLDPE at 190°C.

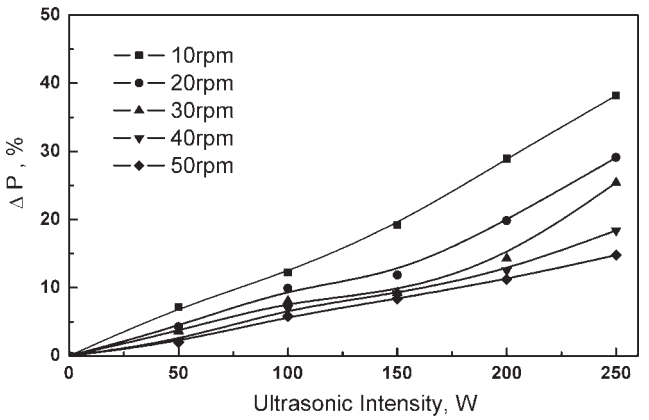

Figure 4 Dependence of relative die pressure reduction of mLLDPE under ultrasonic vibration at various screw rotation speeds at 180°C.

The processing behavior of mLLDPE was greatly enhanced by the incorporation of ultrasonic vibration. At the same ultrasonic intensity, ΔP decreased with the increase in screw rotation speed, indicating that the decrease in die pressure in the presence of ultrasonic vibrations depended on how long the polymer melt was in the die. The lower the screw rotation speed, the longer the polymer melt stayed in the die, and the longer the ultrasonic irradiation of mLLDPE, the higher was the ΔP.

Figure 5 shows the mass flow rate of mLLDPE versus die pressure at different ultrasonic intensities. As shown in Figure 5, the flow rate curves of mLLDPE move upward with an increase in ultrasonic intensity. This means the mass flow rate increased with an increase in ultrasonic intensity at the same die pressure, indicating ultrasonic vibrations can increase the productivity of mLLDPE extrusion.

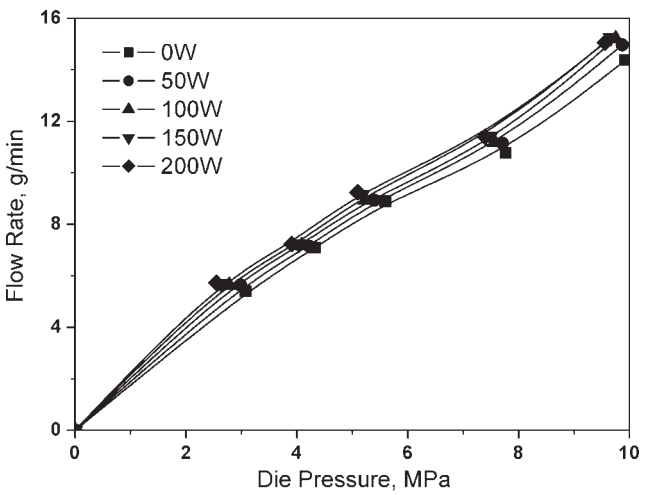

Figure 5 Flow-pressure characteristics of mLLDPE in the presence of ultrasonic vibration with various intensities at 180°C.

Effect of ultrasonic vibration on apparent viscosity of mLLDPE

Figure 6 shows the apparent viscosity curves of mLLDPE during extrusion in the presence and absence of ultrasonic vibrations. As shown in Figure 6, when ultrasonic vibration was applied to mLLDPE extrusion, the apparent viscosity of mLLDPE decreased with an increase in ultrasonic intensity at the same screw rotation speed. When mLLDPE was extruded at a low screw rotation speed (low shear rate), the effect of ultrasonic vibration on reduction in the viscosity of mLLDPE was more obvious because of the long duration of the ultrasonic treatment at a low screw rotation speed. At a shear rate of 46 s^{-1}, the viscosity of mLLDPE decreased from 5895.6 Pa s without ultrasonic vibration to 4898.2 Pa s under 250 W of ultrasonic vibration. The viscosity of mLLDPE was reduced by 17%. Ultrasonic vibrations can promote the motion and disentanglement of polymer chains, causing a reduction in melt viscosity. Therefore, the die pressure and apparent viscosity of mLLDPE in extrusion decreased in the presence of ultrasonic vibrations, showing greater reductions as the ultrasonic intensity increased.

Effect of diatomite/PEG binary processing aid (BPA) on the improvement in processability and the crystallization of mLLDPE

In our previous studies,[20,24,25] we prepared a new type of binary processing aid based on a diatomite/PEG hybrid. This diatomite/PEG binary processing aid exhibited a synergetic effect on viscosity reduction and sharkskin fracture elimination of mLLDPE, as shown in Figures 7 and 8, respectively. The viscosity of mLLDPE/BPA was reduced to 28.1% of that of the

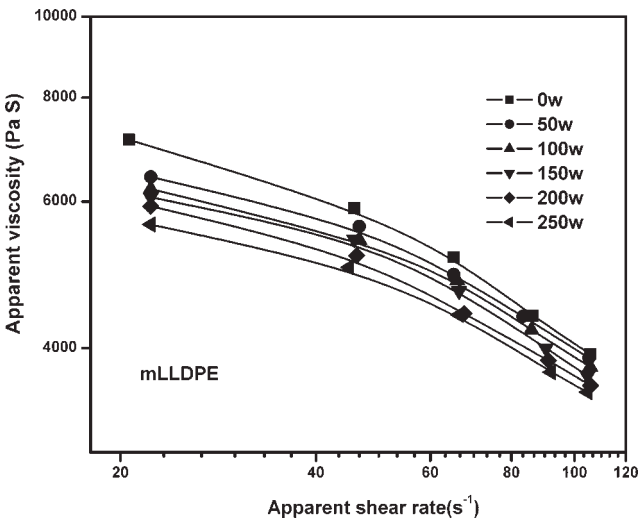

Figure 6 Apparent flow curve of mLLDPE under various ultrasonic intensity.

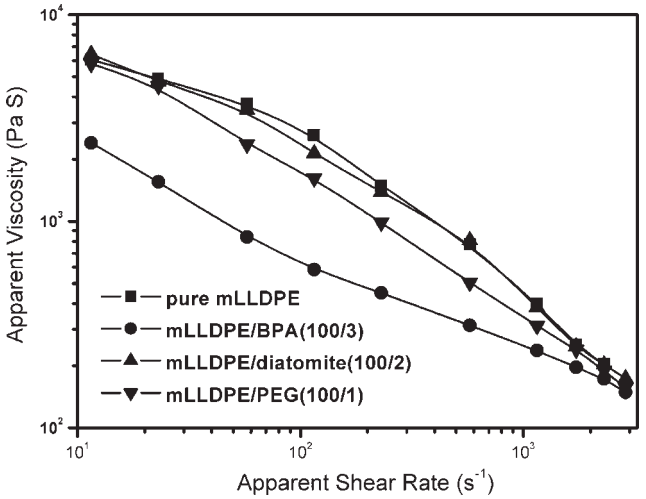

Figure 7 Apparent shear stress versus apparent shear rate for mLLDPE and mLLDPE/additives.

original mLLDPE, and the critical shear rate for the onset of sharkskin fracture of mLLDPE was increased from 230.4 to more than 1152 s^{-1}. Figure 7 shows that the addition of both PEG and BPA decreased the apparent viscosity of mLLDPE. PEG is well known for its low viscosity and lubricating property, which can promote mLLDPE melt slippage on a die wall. Therefore, PEG was expected to cause such a reduction in viscosity for the mLLDPE/PEG blend. However, it is worth noting that BPA showed a synergetic influence on the rheological behavior of mLLDPE. The apparent viscosity of mLLDPE was reduced significantly with the addition of BPA. In general, the introduction of inorganic fillers increases the viscosity of a polymer melt. The incorporation of the diatomite did not decrease the lubricate efficiency of PEG; on the contrary, BPA exhibited a synergetic effect on the reduction of the viscosity of mLLDPE.

Figure 9 shows the surface morphology of mLLDPE/BPA and mLLDPE/PEG extrudates. PEG microdomains were dispersed uniformly on the surface of the original mLLDPE/BPA extrudate, and some fine diatomite particles can be seen in Figure 9(a). After extraction with water for 30 min and then having the water wiped away, the mLLDPE/BPA extrudate was immediately coated with gold for observation. It can be

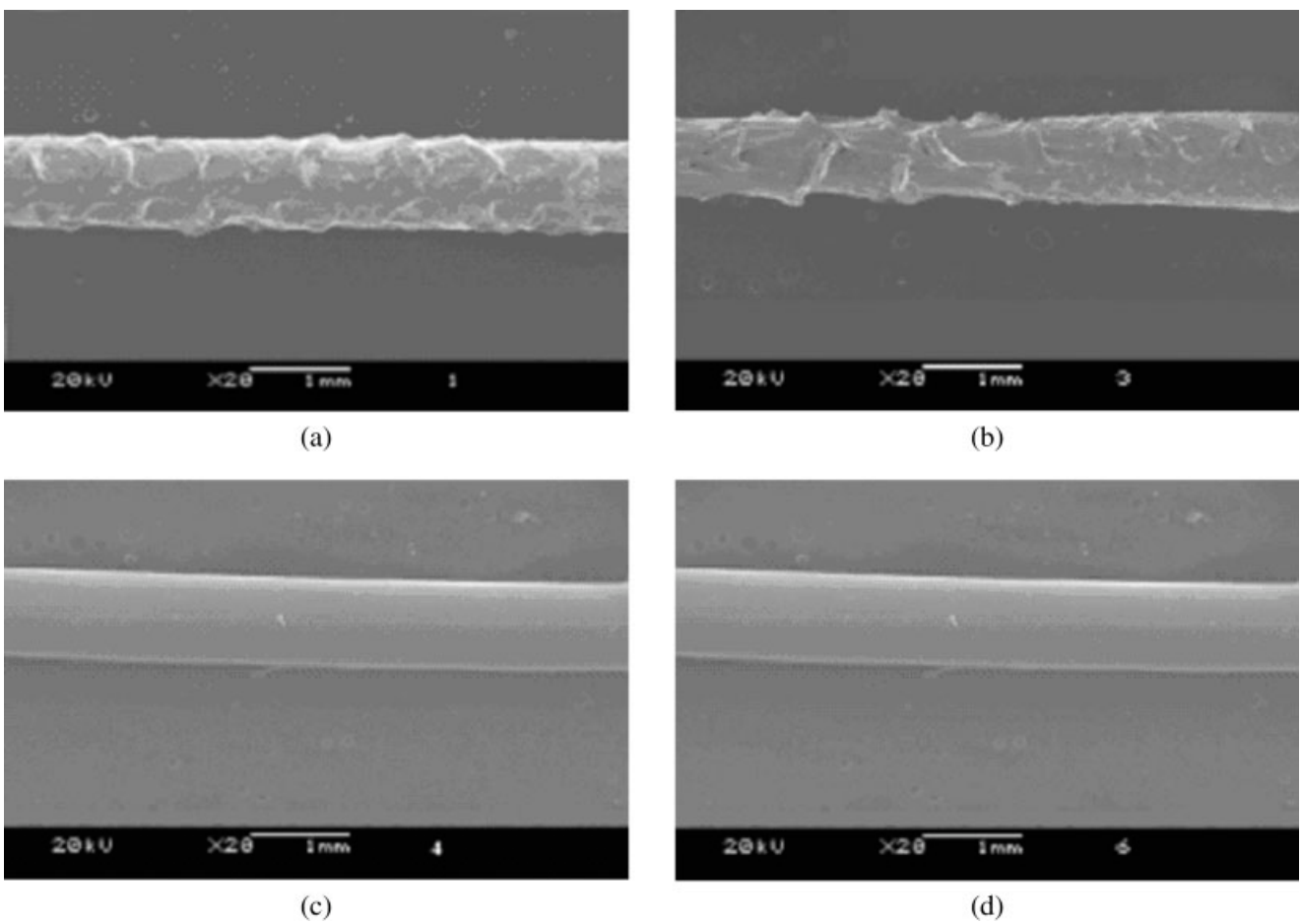

Figure 8 Photographs of extrudate samples of mLLDPE and mLLDPE/BPA: (a) virgin resin at $\gamma = 230.4\ s^{-1}$; (b) virgin resin at $\gamma = 1152\ s^{-1}$; (c) mLLDPE/BPA at $\gamma = 230.4\ s^{-1}$; (d) mLLDPE/BPA at $\gamma = 1152\ s^{-1}$.

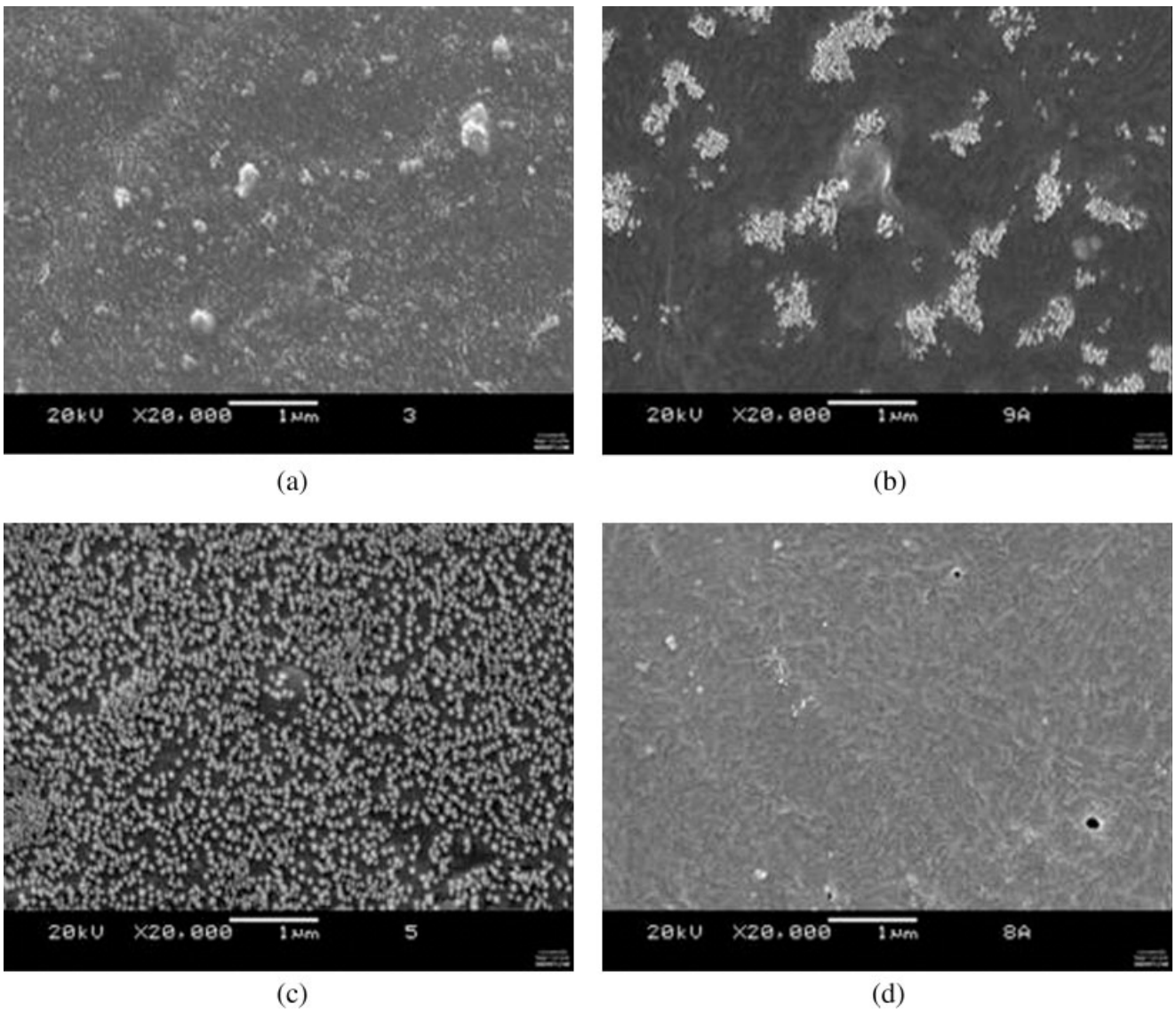

Figure 9 Surface morphology of mLLDPE/BPA and mLLDPE/PEG extrudate: (a) mLLDPE/BPA extrudate; (b) mLLDPE/BPA extrudate coated with gold immediately after extracted with water; (c) mLLDPE/BPA extrudate (placed in a plastic-film bag for 20 h after extracted with water and then coated with gold); (d) mLLDPE/PEG extrudate (placed in a plastic-film bag for 20 h after extracted with water and then coated with gold).

seen from Figure 9(b) that there were still some PEG microdomains dispersed on the surface. This means some PEG microdomains were stuck on the surface of the diatomite fillers because of the strong interaction between the diatomite and PEG. After being extracted with water for 30 min and then having the water wiped away, the mLLDPE/BPA and mLLDPE/PEG extrudates were placed in a plastic-film bag for 20 h and then coated with gold for SEM analysis. For mLLDPE/BPA, a lot of PEG had migrated outside the extrudate and formed PEG microdomains that had dispersed well on the surface of the extrudate. The diameter of the PEG microdomains was smaller than 100 nm [Fig. 9(c)]. However, no PEG microdomains were observed on the extrudate surface of the mLLDPE/PEG blend [Fig. 9(d)].

From the above examination, it can be concluded that, in the extrusion of mLLDPE/PEG, the trend of PEG was to migrate to the die wall because of the low viscosity, that is, most of the PEG was enriched on the surface of the extrudate and the die wall and promoted mLLDPE melt slippage on the die wall. The PEG enriched on the surface of the extrudate was removed after extraction with water. Therefore, no PEG microdomains were observed on the mLLDPE/PEG extrudate surface, even after the extrudate had been placed in a plastic-film bag for 20 h, whereas the motion of the PEG to the wall was disturbed by the diatomite fillers during the extrusion of mLLDPE/BPA and the migration of PEG to the die wall was retarded because of the absorption of the diatomite. Most PEG were coerced to stay in the interior of the extrudates

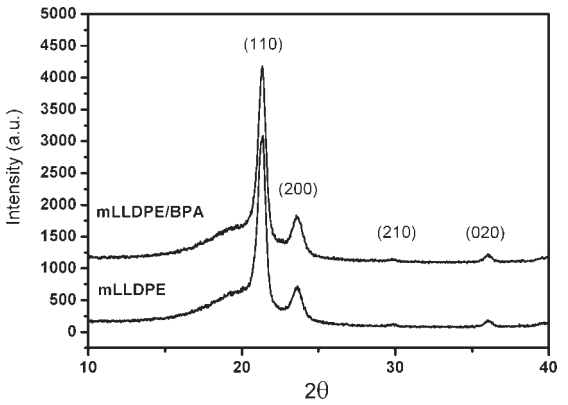

Figure 10 WAXD patterns of mLLDPE and mLLDPE/BPA.

during the extrusion of mLLDPE/BPA. At the same time, under a shear flow field, some of PEG would break away from the diatomite surface or orifice, forming microdomains in the mLLDPE melt. Because of the immiscibility of PEG with polyethylene, the interfacial adhesion is weak between PEG microdomains and the mLLDPE matrix. This part of PEG will act as a flow modifier to promote interfacial slip and to reduce the viscosity of mLLDPE. After the surface of mLLDPE/BPA extrudate was extracted with water, the PEG molecules that stayed inside the extrudate migrated gradually to the extrudate surface, as shown in Figure 9(c).

This analysis shows that the reason BPA reduced the viscosity of mLLDPE melt was not entirely wall slippage on the PEG slip layer. The diatomite of BPA would adsorb most of the PEG component and then suppress the migration of PEG to the interface of the die wall/melt. Consequently, the interfacial slip of mLLDPE melt on the surface of PEG microdomains and the PEG layer coated on diatomite was promoted. The addition of BPA obviously improved the rheological properties of mLLDPE.

In this study, effect of diatomite/PEG binary processing aid (BPA) on the crystallization morphology of mLLDPE was explored by WAXD (Fig. 10). The results are listed in Table II. WAXD analysis showed that the crystallinity and interplanar distance of mLLDPE in the mLLDPE/BPA system changed little compared to pure mLLDPE. DSC analysis also showed the crystallinity of mLLDPE and mLLDPE/BPA are 31.5% and 32.1%, respectively (Table II). This result showed no obvious influence of BPA on the crystallinity of mLLDPE, which accorded well with the results of WAXD.

TABLE II
WAXD Parameters of mLLDPE and mLLDPE/BPA

Sample	D_{110} (nm)	D_{200} (nm)	D_{020} (nm)	X_c (%), WAXD	X_c (%), DSC
mLLDPE	0.4155	0.3752	0.2488	37.6	31.5
mLLDPE/BPA	0.4158	0.3766	0.2493	38.4	32.1

Figure 11 reveals the DSC thermograms of mLLDPE and mLLDPE/BPA at different cooling rates, and the corresponding parameters of the nonisothermal crystallization for mLLDPE and mLLDPE/BPA are listed in Table III. It can be seen that the crystallinity peak of mLLDPE broadened and the crystallinity peak temperature (T_p) moved to a lower temperature with an increase in the cooling rate, which suggests that there was a retardation effect of cooling rate on crystallization for these crystallization processes. These retardation effects resulted from the rate-dependent induction time preceding the initiation of crystallization. Under the same cooling rate, the T_c of mLLDPE/BPA was higher than that of pure mLLDPE. When the

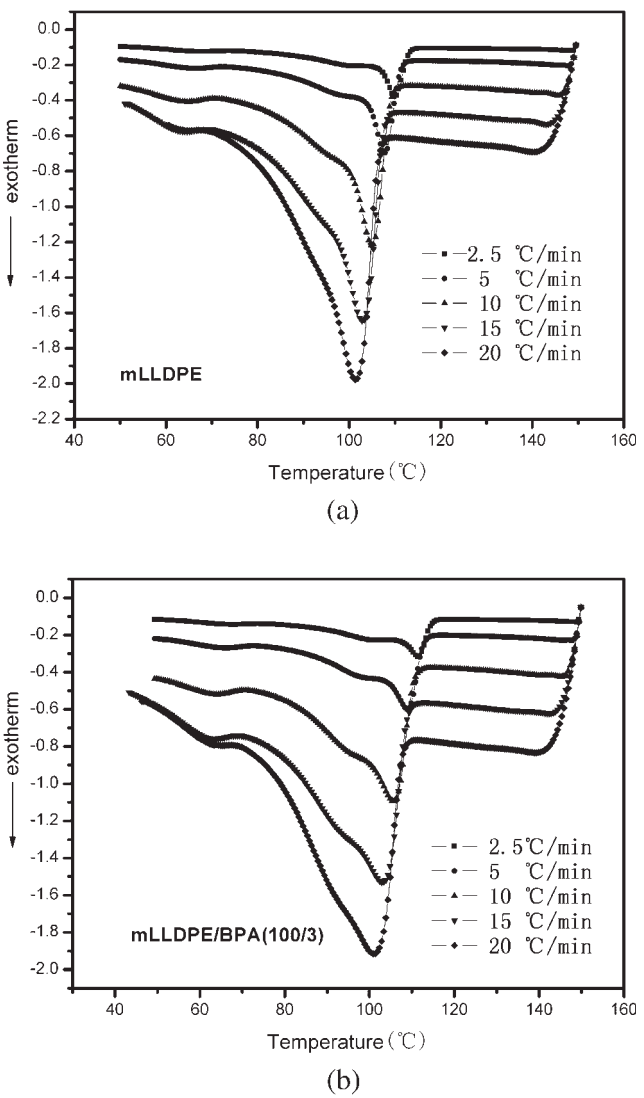

Figure 11 DSC thermograms of mLLDPE and mLLDPE/BPA at different cooling rates.

TABLE III
Nonisothermal Crystallization of mLLDPE and mLLDPE/BPA at Different Cooling Rates

Sample [cooling rate (K/min)]	mLLDPE		mLLDPE/BPA	
	T_m	T_c	T_m	T_c
2.5	122.48	109.97	122.58	111.51
5	121.98	107.77	122.08	108.92
10	121.98	105.05	121.58	105.63
15	121.48	102.92	121.58	103.09
20	—	101.37	—	101.00

hybrid of diatomite/PEG was introduced, the diatomite acted as a nucleating agent, helping to promote the nucleation of mLLDPE; therefore, the T_c of mLLDPE in the mLLDPE/BPA blend increased. At a high cooling rate (20°C/min), the nucleating effect of diatomite was eliminated.

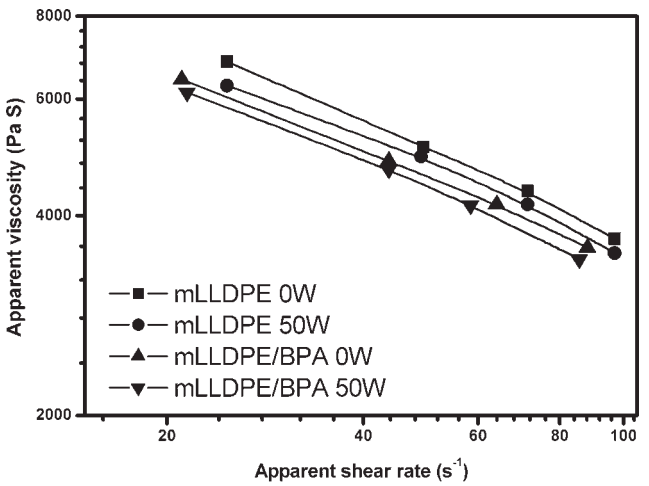

(a)

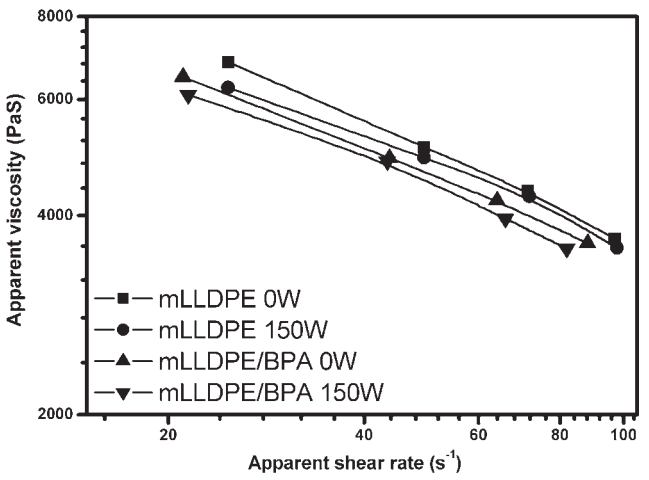

(b)

Figure 12 Apparent viscosity versus apparent shear rate of mLLDPE and mLLDPE/BPA (100 : 0.5) under various ultrasonic intensities.

Synergetic effect of processing aid and ultrasonic vibration on improvement in processability of mLLDPE

The rheological properties of mLLDPE with ultrasonic vibration and binary processing aid applied simultaneously were investigated. As shown in Figures 12 and 13, ultrasonic vibration and binary processing aid exhibited a synergetic effect on viscosity reduction of mLLDPE. The combination of ultrasonic vibration and binary processing aid further improved the processability of mLLDPE compared to either ultrasonic vibration or binary processing aid used individually. At a shear rate of 50.08 s^{-1}, the viscosity of mLLDPE extruded with ultrasonic intensity of 150 W was reduced to 93% of that without ultrasonic vibration. With the combination of ultrasonic vibration and a small amount of binary processing aid, the viscosity of mLLDPE was reduced to 85.3% of that without the application of ultrasonic vibration and binary processing aid. The results indicated that there was a synergetic effect of processing aid and ultrasonic vibration in improving the processability of mLLDPE.

Figure 13 shows the effect of ultrasonic vibration and binary processing aid on the extrudate swell ratio of mLLDPE. The reduction of the extrudate swell ratio of mLLDPE increased with an increase in ultrasonic intensity. With the introduction of ultrasonic vibrations, the mobility and disentanglements of the polymer chain were activated. The relaxation process of the polymer chain was shortened, which caused a reduction in melt viscosity and elasticity. With the combination of ultrasonic vibration and a small amount of BPA applied, the extrudate swell ratio of mLLDPE was reduced further.

Effect of ultrasonic vibration on the mechanical properties of mLLDPE/BPA

The effect of ultrasonic vibration at different intensities and BPA on the mechanical properties of mLLDPE was

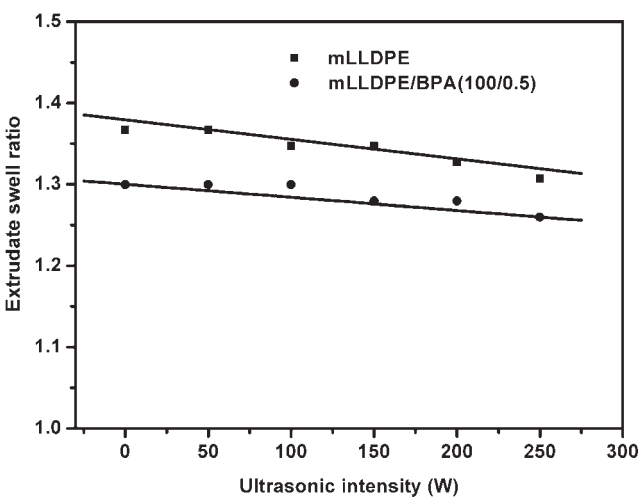

Figure 13 Effect of ultrasonic vibration and BPA on the extrudate swell ratio of mLLDPE (rotational speed: 20 rpm).

TABLE IV
Mechanical Properties of mLLDPE and mLLDPE/BPA (100 : 0.5) under Various Ultrasonic Intensities

Samples	Ultrasonic intensity (W)	Elongation at break (%)	Strength at break (MPa)	Yield strength (MPa)
mLLDPE	0	666	31	11
	50	656	31	11
	100	655	29	11
	150	638	30	11
	200	666	32	12
	250	641	31	12
mLLDPE/BPA	0	647	29	11
	50	653	30	11
	100	629	30	11
	150	659	32	12
	200	640	31	12

studied, as shown in Table IV. The experimental results showed that ultrasonic vibration had a slight effect on the mechanical properties of mLLDPE and mLLDPE/BPA. It was expected that ultrasonic vibration technology would be an effective processing method. With the application of ultrasonic vibrations and BPA, the mechanical properties of mLLDPE did not worsen, whereas the processability of mLLDPE was obviously enhanced.

CONCLUSIONS

The processability of mLLDPE was studied with the application of ultrasonic vibration and binary processing aid. The die pressure and apparent viscosity of mLLDPE were reduced in the presence of ultrasonic vibration. With the increase in ultrasonic intensity, there were further reductions in die pressure and apparent viscosity. The effect of ultrasonic vibration on sharkskin fracture of mLLDPE was marginal. Diatomite/PEG binary processing aid decreased the viscosity and increased the critical shear rate for the onset of sharkskin fracture, enhancing the processing efficiency of mLLDPE. The combination of ultrasonic vibration and binary processing aid further improved the processability of mLLDPE. In this way, mLLDPE resins could be processed at a lower processing temperature with low die pressure and energy consumption. The crystallinity and the crystal plane spacing of mLLDPE in the mLLDPE/BPA system changed slightly compared to those of pure mLLDPE. The introduction of BPA promoted the nucleation of mLLDPE and the growth of the crystal.

REFERENCES

1. Kim, Y. S.; Chung, C. I.; Lai, S. Y.; Hyun, K. S. J Appl Polym Sci 1996, 59, 125.
2. Munoa-Escalona, A.; Lafuente, P.; Vega, J. F.; Santamaria, A. Polym Eng Sci 1999, 39, 2292.
3. Yan, D.; Wang, W. J.; Zhu, S. Polymer 1999, 40, 1737.
4. Starck, P.; Malmberg, A.; Lofgren, B. J Appl Polym Sci 2002, 83, 1140.
5. Liu, C.; Wang, J.; He, J. Polymer 2002, 43, 3811.
6. Kwag, H. J.; Rana, D.; Cho, K.; Rhee, Y. W.; Woo, T.; Lee, B. H. Polym Eng Sci 2000, 40, 1672.
7. Vega, J. F.; Santamaria, A.; Munoa-Escalona, A.; Lafuente, P. Macromolecules 1998, 31, 3639.
8. Wood-Adams, M. P.; Dealy, J. M. Macromolecules 2000, 33, 7489.
9. Claus, G.; Munstedt, H. Rheol Acta 2002, 41, 232.
10. Han, C. D. Rheology in Polymer Processing; Academic Press: New York, 1976.
11. Xing, K. C.; Schreiber, H. P. Polym Eng Sci 1996, 36, 337.
12. Eonseok, L.; White, J. L. Polym Eng Sci 1999, 39, 327.
13. Migler, K. B.; Lavallee, C.; Dillon, M. P.; Wooda, S. S.; Gettinger, C. L. J Rheol 2001, 45, 565.
14. Migler, K. B.; Son, Y.; Qiao, F.; Flynn, K. J Rheol 2002, 46, 383.
15. Rosenbaum, E. E.; Randa, S. K.; Hatzikiriakos, S. G.; Stewart, C. W.; Henry, D. L.; Buckmaster, M. Polym Eng Sci 2001, 40, 179.
16. Seth, M.; Hatzikiriakos, S. G.; Clere, T. M. Polym Eng Sci 2002, 42, 743.
17. Kazatchkov, I. B.; Yip, F.; Hatzikiriakos, S. G. Rheol Acta 2002, 39, 583.
18. Seth, M.; Hatzikiriakos, S. G. J Vinyl Addit Technol 2001, 7, 90.
19. Myung, L. S.; Kim, J. G. J Vinyl Addit Technol 2002, 8, 118.
20. Liu, X.; Li, H. J Appl Polym Sci 2004, 93, 1546.
21. Isayev, A. I.; Wong, C. M.; Zeng, X. SPE ANTEC Tech Paper 1987, 33, 207.
22. Isayev, A. I.; Wong, C. M.; Zeng, Z. Adv Polym Technol 1990, 10, 31.
23. Liu, G.; Li, H. J Appl Polym Sci 2003, 89, 2628.
24. Liu, X. L.; Li, H. L. Polym Eng Sci 2005, 45, 898.
25. Liu, X. L.; Li, H. L. J Appl Polym Sci 2005, 96, 1824.